IEEE Access
Multidisciplinary | Rapid Review | Open Access Journal

Received July 13, 2020, accepted August 7, 2020, date of publication August 21, 2020, date of current version September 9, 2020.

*Digital Object Identifier 10.1109/ACCESS.2020.3018474*

# Channel Estimation Based on Adaptive Denoising for Underwater Acoustic OFDM Systems

**YONG-HO CHO AND HAK-LIM KO**
Department of Information and Communication Engineering, Hoseo University, Asan 31499, South Korea

Corresponding author: Hak-Lim Ko (hlko@hoseo.edu)

This work was supported in part by the project titled "Development of Distributed Underwater Monitoring and Control Networks", funded by the Ministry of Oceans and Fisheries, Korea, and in part by the MSIT(Ministry of Science and ICT), Korea, under the ITRC(Information Technology Research Center) support program(IITP-2020-2018-0-01417) supervised by the IITP(Institute for Information & communications Technology Promotion).

**ABSTRACT** Underwater acoustic (UWA) communications systems suffer from a low signal-to-noise ratio (SNR) and a doubly selective channel, which are caused by many limitations, such as high propagation loss, slow propagation speed, and time-varying environmental factors. To overcome a low SNR, various diversity techniques are often adopted in UWA communications. However, such diversity can only be exploited with knowledge of the channel. Accordingly, channel estimation needs to be performed without obtaining the benefit of diversity. Moreover, accurate side information that can support a channel estimator (CE) is difficult to acquire at a low SNR under doubly selective channel. In this article, a novel CE based on an adaptive denoising is proposed for UWA orthogonal frequency-division multiplexing (OFDM) systems. The proposed method exploits two different types of pilot symbols. Channel impulse response (CIR) is estimated based on primary pilot symbols. By minimizing the squared error of the received secondary pilot symbols, a near-optimal denoising window is adaptively determined based on the channel length for the given CIR estimate. The proposed method does not require a priori information about channel statistics and SNR values. Analysis on the effect of denoising and the performance of the proposed denoising window estimator are also presented. Simulation and at-sea experiments verify that the proposed method has superior performance, compared with conventional CEs over diverse channel conditions. Complexity analysis shows that the proposed method is computationally efficient. Therefore, the proposed method is effective for real-time UWA OFDM systems under a harsh UWA channel with strong noise.

**INDEX TERMS** Adaptive denoising, channel estimation, experiment, orthogonal frequency division multiplexing (OFDM), underwater acoustic communications.

## I. INTRODUCTION

Recently, underwater wireless communications systems have received substantial attention because it is essential to facilitate new applications, such as underwater environment monitoring, undersea rescues, deep sea mining, and so on. Various media (e.g., acoustic [1], [2], optical [3], and magnetic induction [4]) have been researched to offer wireless communications in the underwater environment. Among these, an acoustic wave has been known to provide wide-area connectivity due to the relatively good propagation characteristics, compared with other media.

The associate editor coordinating the review of this manuscript and approving it for publication was Qingchun Chen.

Although acoustic wave is preferred for underwater wireless communications systems, it suffers from many limitations, such as reflections, high propagation loss, slow propagation speed, and so on [5]. In particular, an acoustic signal is well reflected by the bottom and the surface of water, which causes many multipaths with long delays. Due to the slow propagation speed, the Doppler effect can easily occur with the acoustic signal. Moreover, the underwater channel varies over time due to many environmental factors, such as wind, tidal currents, oceanic tides, and so on. Accordingly, underwater acoustic (UWA) communications experiences a time-varying doubly selective channel. Note that those limitations yield a much larger impact on system performance, compared with terrestrial radio frequency-based communications. Consequently, it is very challenging to achieve

a reliable and high-speed link with UWA communications systems.

Another factor that makes UWA communications challenging is the high propagation loss of the acoustic wave. The acoustic wave experiences absorption and spreading loss, which increase with frequency and distance, respectively [6]. As a result, the received signal strength is typically very weak, and, therefore, a typical UWA communications link is established in a low signal-to-noise ratio (SNR) regime.

To combat the harsh underwater channel, orthogonal frequency division multiplexing (OFDM) with a cyclic prefix (CP), which is a multicarrier transmission technology, has been widely applied in UWA communications systems in recent years. The CP-OFDM system has many advantages over conventional single-carrier systems, including robustness against a multipath channel, high spectral efficiency, as well as the feasibility of low-cost transceiver implementations [7]. Robustness against a multipath channel comes from the fact that the CP-OFDM system is able to convert a multipath channel in the time domain into a one-tap response for each subcarrier in the frequency domain. In order to guarantee successful equalization and the data decoding, therefore, accurate channel estimation is indispensable for the CP-OFDM system.

Many channel estimators (CEs) have been proposed for the UWA CP-OFDM system [8]–[16]. Unless channel bandwidth is narrow, the UWA channel is known to have resolvable sparse paths. In order to exploit sparsity of the channel, many recent methods have been devised based on the principle of compressed sensing (CS). In [8], basis pursuit (BP) and orthogonal matching pursuit (OMP) methods, which are the most popular recovery algorithms for CS technology, were adopted for estimating time-varying UWA channels. It was shown in [8] that CS-based channel estimation is effective for sparse time-varying UWA channel. To enhance reconstruction performance over the OMP method, a compressive sampling matching pursuit (CoSaMP) algorithm was applied for UWA channel estimation [11]. The OMP and CoSaMP algorithms require the sparsity level of the channel as a priori information. To resolve such a restriction, a sparsity adaptive CoSaMP based on a dynamic threshold and weak selection of atoms (DW-SACoSaMP) was proposed in [15]. Along with sparsity adaptation, this algorithm offers reduced complexity.

However, the above CEs have poor estimation performance in a low SNR regime, and exhibit their gain only at a high SNR. The simple way to overcome the low received SNR is to increase transmission power. Considering that communication nodes in UWA communications systems are energy-constrained, however, boosting power can limit the network life span substantially. In order to overcome a low SNR, diversity is often exploited in the spatial, temporal, and spectral domains. A typical way to achieve spatial diversity is to employ multiple receiving hydrophones [8], [17], [18]. Temporal and spectral diversity can easily be exploited by transmitting data repeatedly in time and frequency domains. However, gain in diversity can be obtained with information about the channel, and, subsequently, the channel estimation needs to be performed without obtaining the benefit of diversity.

At a low SNR, the received pilot symbols contain a large amount of noise. In such a regime, it is crucial for the CE to mitigate the noise for accurate estimation performance. To mitigate noise in channel estimation, many denoising techniques have been proposed for CP-OFDM systems [19]–[21]. The denoising technique discards noise components from a channel impulse response (CIR) estimate based on a threshold, thereby reducing the noise effect on the subsequent estimation of channel frequency response (CFR). In [19], a threshold is derived based on an optimality condition, which is equal to twice the noise variance. In [20], a threshold is derived based on a more elaborated condition, which requires channel length, number of actual channel taps and the noise variance a priori.

The thresholds in most denoising techniques are determined based on the received SNR value [22]. Due to the time-varying nature of the UWA channel, however, accurate estimation of the SNR value may not be available prior to threshold estimation. Moreover, a low-value SNR is difficult to estimate under highly frequency-selective channels [23]. A wrong threshold caused by inaccurate SNR estimate can discard the actual channel tap, and/or fail to discard noise components, both of which will significantly degrade the performance of channel estimation.

In this article, a novel CE based on an adaptive denoising technique is proposed for UWA CP-OFDM system in order to overcome a harsh UWA channel with strong noise. The proposed method exploits two different types of pilot symbols: the first is used for estimation of the CIR and CFR, while the second is used to adaptively determine the denoising window for the given CIR estimate. In particular, the proposed method yields a near-optimal denoising window by minimizing the squared error (SE) of the received secondary pilot symbols without a priori information about channel statistics and SNR values. The effect of denoising and the performance of the proposed denoising window estimator are analyzed from the perspective of mean squared error (MSE). It is demonstrated through simulation and at-sea experiments that the proposed method outperforms conventional CEs [8], [15], [24] under diverse UWA channels. Furthermore, it is shown by complexity analysis that the proposed method can be realized with much less complexity, compared with the conventional CS-based CEs.

The rest of this article is structured as follows. In Section II, the system model is explained. The proposed channel estimation method and a performance analysis are presented in Section III and IV, respectively. Performance evaluations based on the simulation and the experimental results are described in Section V and VI, respectively. Conclusions are drawn in Section VII.

*Notations*: $\mathbf{I}_K$ is a $K \times K$ identity matrix. $[\mathbf{x}]_i$ and $[\mathbf{Y}]_{i,j}$ denote the $i$-th entry of the vector $\mathbf{x}$ and the $(i, j)$-th entry of the matrix $\mathbf{Y}$, respectively. $|\mathcal{I}|$ is the cardinality of set $\mathcal{I}$.

$D(\cdot)$ denotes a diagonalization operation. $\text{col}_l(\mathbf{X})$ and $\text{row}_l(\mathbf{X})$, respectively, are the $l$-th column and row vector of $\mathbf{X}$.

## II. SYSTEM MODEL

We consider a CP-OFDM with $N$ subcarriers, among which $N_U$ subcarriers are active for transmission of data and pilot symbols, while $N_G$ subcarriers are inactive for guard bands; i.e., $N = N_U + N_G$. The transmission of information data is on a time-frame basis, where a frame consists of $N_{preamble}$ preambles at the beginning followed by $N_{sym}$ OFDM symbols. Note that all OFDM symbols belonging to a frame need to be processed to recover the transmitted information.

Let $\mathbf{S}_i = [S_i(0),\ S_i(1),\ \cdots,\ S_i(N-1)]^T$ denote the modulated symbols on $N$ subcarriers of the $i$-th OFDM symbol. The first and last $N_G/2$ symbols of $\mathbf{S}_i$, which correspond to the guard bands at each edge of the spectrum, are 0. Among the $N_U$ symbols, $N_{DC}$ symbols around the middle of the spectrum are set to 0 for direct current (DC). The remaining symbols of $\mathbf{S}_i$ are reserved for data and pilot symbols. The time-domain sample of the $i$-th OFDM symbol $s_i[n]$ is then given by

$$s_i[n] = \frac{1}{\sqrt{N}} \sum_{k=0}^{N-1} S_i(k) e^{j\frac{2\pi}{N}kn}, \quad n = 0,\ \cdots,\ N-1. \tag{1}$$

Before transmission, a CP of length $N_{cp}$ samples is appended to the beginning of each OFDM symbol to preserve orthogonality between subcarriers on the receiver side. After CP insertion, the time-domain samples are pulse-shaped and up-converted to carrier frequency $f_c$. The transmitted signal in the passband is given by

$$\tilde{s}(t) = 2\text{Re}\left( \sum_{i=0}^{N_{sym}-1} \sum_{n=-N_{cp}}^{N-1} s_i[n] q\left(t - (iN_b + n)\, T_s\right) \right) e^{j2\pi f_c t} \tag{2}$$

where $q(t)$ is a pulse-shaping filter, $N_b = N + N_{cp}$, and $T_s$ denotes the sample duration.

In UWA communications systems, the transmitted signal undergoes a multipath channel in which each channel tap experiences time-varying delay and path gain. Many factors can cause time variation of the channel, such as motion of the transmitter and receiver, scattering by the moving sea surface, and refraction due to sound speed variations [8]. It can be assumed that within the duration of an OFDM symbol, the path gain of the channel taps is constant, while its delay is time-varying by the Doppler rate, as follows [8]:

$$\tau_l(t) = \tau_l - a_l t, \tag{3}$$

where $a_l$ is the Doppler rate for the $l$-th channel tap. Then, the CIR is defined as follows [17]:

$$c(\tau,\ t) = \sum_{l=0}^{N_{path}-1} A_l\, \delta\left(\tau - \tau_l + a_l t\right) \tag{4}$$

where $N_{path}$ and $A_l$ denote the number of channel taps and the path gain of the $l$-th channel tap, respectively. Lastly, the received signal in the passband can be written as

$$y(t) = \sum_{l=0}^{N_{path}-1} A_l\, \tilde{s}(t - \tau_l + a_l t) + w(t) \tag{5}$$

where $w(t)$ is additive white Gaussian noise (AWGN) with a zero mean and variance $\sigma_n^2$.

In this article, we consider that the transmitter and receiver to be installed in a fixed location, or they are merely drifting. Under such circumstances, the Doppler effect is limited. We also adopt a two-step approach to the received signal prior to channel estimation: resampling in the passband based on the estimated Doppler scale, followed by Doppler shift compensation [8]. Accordingly, a residual Doppler rate in the resultant received signal can be assumed to be small. Ignoring the residual Doppler rate for ease of derivation (i.e., $a_l = 0,\ \forall l$), the CIR in (4) can then be simplified to the well-known time-invariant tapped-delay-line model, as follows:

$$h(\tau) = \sum_{l=0}^{N_{path}-1} A_l\, \delta\left(\tau - \tau_l\right) \tag{6}$$

Let $\mathbf{h} = [h(0),\ h(1),\ \cdots,\ h(N-1)]^T$ denote a time-invariant $N \times 1$ CIR vector with covariance matrix $\mathbf{C}_h = E[\mathbf{h}\mathbf{h}^H]$, which contains an actual CIR of length $L_h$. The $N_U \times 1$ received symbol vector carried by the $i$-th OFDM symbol is given by

$$\mathbf{y}_i = \sqrt{N} D\left(\mathbf{S}_i\right) \mathbf{F}\mathbf{h} + \mathbf{F}\mathbf{w} \tag{7}$$

where $\mathbf{F}$ is an $N \times N$ discrete Fourier transform (DFT) matrix with entries $[\mathbf{F}]_{m,\,n} = \frac{1}{\sqrt{N}} e^{-j\frac{2\pi}{N}mn}$, and $\mathbf{w}$ is an AWGN vector.

## III. PROPOSED CHANNEL ESTIMATION METHOD

### A. PILOT ALLOCATION

For the proposed CE, two types of pilot symbols allocated in a comb-type fashion are employed. The first type of pilot, denoted as a primary pilot symbol (PPS), is used for estimation of the CIR and the corresponding CFR. The second type of pilot, denoted as a secondary pilot symbol (SPS), is used to estimate an adaptive denoising window for noise reduction.

In the considered system, the PPSs are each allocated at every $D_f$-th subcarrier and $D_t$-th OFDM symbol. Let $I_f$ and $I_t$ denote the indices of the subcarrier and the OFDM symbol of the PPSs, respectively, while $N_p = |I_f|$ and $N_t = |I_t|$ denote the number of PPSs in the frequency and time domain, respectively. Likewise, the SPSs are each allocated at every $\bar{D}_f$-th subcarrier and $\bar{D}_t$-th OFDM symbol. Let $\bar{I}_f$ and $\bar{I}_t$ respectively denote the indices of the subcarrier and the OFDM symbol for the SPSs, and $\bar{N}_p = |I_f|$ and $\bar{N}_t = |I_t|$ denote the number of SPSs in the frequency and time domain, respectively. It is worth noting that SPSs is allocated far more sparsely than PPSs, because they are used only for denoising window estimation. Without loss of generality, both the PPS and SPS are assumed to have a constant amplitude equal to 1.

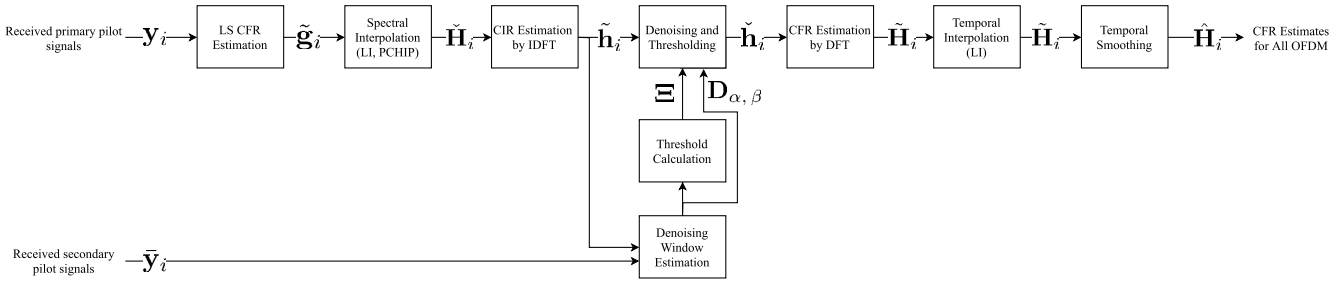


**FIGURE 1.** Block diagram of the proposed CE method.

### B. CFR ESTIMATION

In UWA communications systems, received signals are very noisy due to the large propagation loss and the many noise sources. Consequently, channel estimation is performed under the existence of strong noise. Furthermore, the underwater channel has a large variation in channel length. To minimize the noise effect and enhance estimation accuracy in such circumstances, therefore, a CFR estimation method with an adaptive denoising technique is proposed, wherein the denoising window is adaptively determined based on the channel length without a priori information. The proposed method makes use of both PPS and SPS. In Fig. 1, the procedure of the proposed method is illustrated.

The received PPSs in the $i$-th OFDM symbol can be written in an $N_p \times 1$ vector form as

$$\mathbf{y}_i = \sqrt{N}\mathbf{X}_i\mathbf{B}\mathbf{h} + \mathbf{B}\mathbf{w}, \quad i \in I_t \tag{8}$$

where $\mathbf{X}_i$ is an $N_p \times N_p$ diagonal matrix in which the $k$-th element is the $k$-th PPS of the $i$-th OFDM symbol, and $\mathbf{B}$ is an $N_p \times L_h$ DFT matrix with entries $[\mathbf{B}]_{m,n} = \frac{1}{\sqrt{N}} e^{-j\frac{2\pi}{N} I_f(m)n}$. The least-square (LS) estimation of the CFR at the subcarriers carrying the PPSs in the $i$-th OFDM symbol is given by

$$\tilde{\mathbf{g}}_i = \mathbf{X}_i^H \mathbf{y}_i, \quad i \in I_t \tag{9}$$

where $\mathbf{X}_i^H \mathbf{X}_i = \mathbf{I}_{N_p}$ is assumed.

Based on the LS CFR estimate $\tilde{\mathbf{g}}_i$, the CFR estimate vector over all the useful subcarriers $\tilde{\mathbf{H}}_i$ is obtained via interpolation technique in the frequency domain. Several spectral interpolation techniques [24] have been studied for channel estimation in OFDM systems: linear interpolation (LI), piecewise cubic Hermite interpolation (PCHIP), and spline interpolation. In this article, LI and PCHIP techniques are considered. The CFR estimate at the $k$-th subcarriers $[\tilde{\mathbf{H}}_i]_k$ for $I_f(m) < k < I_f(m+1)$ is given by

$$[\tilde{\mathbf{H}}_i]_k = \left[\tilde{\mathbf{g}}_i\right]_m + \left(\left[\tilde{\mathbf{g}}_i\right]_{m+1} - \left[\tilde{\mathbf{g}}_i\right]_m\right) c_1 + c_2 + c_3 \tag{10}$$

where, for the LI technique,

$$\begin{aligned} l &= k - I_f(m), \quad c_0 = l/D_f, \\ c_1 &= c_0, \quad c_2 = c_3 = 0 \end{aligned} \tag{11}$$

and for the PCHIP technique,

$$\begin{aligned} l &= k - I_f(m), \quad c_0 = l/D_f, \\ c_1 &= 3c_0^2 - 2c_0^3, \\ c_2 &= l\,(c_0 - 1)^2\, d_m, \quad c_3 = lc_0\,(c_0 - 1)\, d_{m+1}, \end{aligned} \tag{12}$$

and $d_m$ is the slope of the interpolant at $I_f(m)$ [24]. Note that the CFR estimation with LI technique can be represented in a matrix form as

$$\check{\mathbf{H}}_i = \Gamma\tilde{\mathbf{g}} = \Gamma\mathbf{X}_i^H\mathbf{y}_i, \quad i \in I^t \tag{13}$$

where $\Gamma$ is an $N_U \times N_p$ linear-interpolation matrix of which the $(m,n)$-th entry is

$$[\Gamma]_{m,n} = \begin{cases} (I_f(n+1) - m)/D_f, \\ \text{for } m \in I_f, n = \underset{n}{\text{argfirst}}\{I_f(n+1) > m\} \\ \left(m - I_f(n)\right)/D_f, \\ \text{for } m \in I_f, n = \underset{n}{\text{argfirst}}\{I_f(n) > m\} \\ 0, \quad \text{otherwise} \end{cases} \tag{14}$$

The noisy CIR estimate for the $i$-th OFDM symbol is obtained by transforming CFR estimate $\check{\mathbf{H}}_i$ into the time domain through an inverse DFT operation as

$$\tilde{\mathbf{h}}_i = \frac{1}{\sqrt{N}}\mathbf{Q}^H\check{\mathbf{H}}_i, \quad i \in I_t \tag{15}$$

where $\mathbf{Q}$ is an $N_U \times N$ DFT matrix with entries $[\mathbf{Q}]_{m,n} = \frac{1}{\sqrt{N}} e^{-j\frac{2\pi}{N} I_U(m)n}$, and $I_U$ is the indices of the $U$ active subcarriers.

CIR estimate vector $\tilde{\mathbf{h}}_i$ has a length equal to $N$, which is far larger than the maximum excess delay (MED) of the channel. This means that most of the elements in $\tilde{\mathbf{h}}_i$ correspond to unwanted noise. In UWA communications systems, the MED of the UWA channel changes over time due to environmental variations. Considering the intermittent transmission nature of UWA communications, it is difficult to acquire information on the MED prior to channel estimation. Therefore, a key role of channel estimation in UWA communications systems is to determine the actual CIR region and to discard the noise from a noisy CIR estimate without knowing the MED.

For effective noise suppression, a two-step approach exploiting the SPS is proposed: adaptive denoising followed by thresholding. Adaptive denoising is first applied to noisy CIR estimates in order to remove the noise outside of the actual CIR region. Since this noise region consists of most of the noise in the CIR estimates, adaptive denoising is very

effective at noise suppression, especially at a low SNR. In the proposed method, a denoising window is determined in a adaptive way based on the SPSs, which will be discussed in the following subsection. Thresholding is then performed to discard residual noise within the actual CIR region.

Let $\mathbf{D}_{\alpha,\beta}$ denote an $N \times N$ diagonal denoising window matrix as

$$\left[\mathbf{D}_{\alpha,\beta}\right]_{k,k} = \begin{cases} 0, & \text{for } \alpha \le k \le \beta \\ 1, & \text{otherwise} \end{cases} \tag{16}$$

where $\alpha$ and $\beta$ of $\mathbf{D}_{\alpha,\beta}$ represent the start and end indices of the denoising window, respectively. Let $\Xi$ denote an $N \times N$ diagonal matrix that selects the actual channel taps based on a threshold as

$$[\Xi]_{k,k} = \begin{cases} 1, & \left|\left[\tilde{\mathbf{h}}_i\right]_k\right|^2 > \gamma\tilde{\sigma}_n^2 \\ 0, & \text{otherwise.} \end{cases} \tag{17}$$

Note that noise variance estimate $\sigma_n^2$ can be obtained based on the denoising window as

$$\tilde{\sigma}_n^2 = \frac{1}{\beta - \alpha + 1}\sum_{k=\alpha}^{\beta}\left|\left[\tilde{\mathbf{h}}_i\right]_k\right|^2. \tag{18}$$

By applying denoising $\mathbf{D}_{\alpha,\beta}$ followed by the thresholding with $\Xi$, the noise can be eliminated effectively from the CIR estimate. The noise-suppressed CIR estimate is given by

$$\check{\mathbf{h}}_i = \Xi\mathbf{D}_{\alpha,\beta}\tilde{\mathbf{h}}_i, \quad i \in I_t. \tag{19}$$

The refined CFR estimate over the useful subcarriers for the $i$-th OFDM symbol can now be obtained from the noise-suppressed CIR estimate through the DFT operation as

$$\check{\mathbf{H}}_i = \sqrt{N}\mathbf{Q}\check{\mathbf{h}}_i, \quad i \in I_t. \tag{20}$$

If the PPSs are not allocated to all OFDM symbols in a frame ($D_t > 1$), a temporal interpolation technique such as LI can be applied to acquire the CFR estimate for the OFDM symbol not carrying the pilots as

$$\check{\mathbf{H}}_j = (\check{\mathbf{H}}_{i+D_t} - \check{\mathbf{H}}_i)\frac{j-i}{D_t} + \check{\mathbf{H}}_i, \quad i < j < i + D_t,\ i \in I_t. \tag{21}$$

For further noise reduction, the CFR estimates for all OFDM symbols in a frame are then smoothed by adaptive temporal filtering as

$$\check{\mathbf{H}}_i = (1-\lambda)\check{\mathbf{H}}_{i-1} + \lambda\check{\mathbf{H}}_i, \quad i = 1, 2, \cdots, N_{sym}-1. \tag{22}$$

where $\lambda \in [0, 1)$ accounts for the filter memory. A lower value for the $\lambda$ will provide more noise reduction, but is more susceptible to channel variation, and vice versa.

### C. THE SPS-AIDED DENOISING WINDOW ESTIMATION

In the proposed CE, the denoising window is determined in order to minimize the SE of the received SPS. Based on the noisy CIR estimates $\tilde{\mathbf{h}}_i$ for the given $\mathbf{D}(\alpha, \beta)$, a tentative CFR estimates at the subcarriers of the SPSs in the $i$-th OFDM symbol can be obtained as

$$\bar{\mathbf{H}}_i(\alpha, \beta) = \sqrt{N}\bar{\mathbf{B}}\mathbf{D}(\alpha, \beta)\tilde{\mathbf{h}}_i, \quad i \in \bar{I}_t \tag{23}$$

where $\bar{\mathbf{B}}$ is an $\bar{N}_p \times N$ DFT matrix with entries $[\bar{\mathbf{B}}]_{m,n} = e^{-j\frac{2\pi}{N}\bar{I}_f(m)n}$. Here, it is assumed for ease of derivation that the PPS-bearing OFDM symbols also carry the SPSs (i.e., $\bar{I}_t \in I_t$).[1] For a given $\alpha$ and $\beta$, let $\varepsilon_i$ denote the SE of the received SPSs in the $i$-th OFDM symbol as

$$\begin{aligned}\bar{\varepsilon}_i(\alpha, \beta) &= \frac{1}{\bar{N}_p}||\bar{\mathbf{y}}_i - \bar{\mathbf{X}}_i\bar{\mathbf{H}}_i(\alpha, \beta)||_2^2 \\ &= \frac{1}{\bar{N}_p}||\bar{\mathbf{X}}_i^H\bar{\mathbf{y}}_i - \bar{\mathbf{H}}_i(\alpha, \beta)||_2^2\end{aligned} \tag{24}$$

where $\bar{\mathbf{y}}_i$ denotes the received SPSs in the $i$-th OFDM symbol, and $\bar{\mathbf{X}}_i$ denotes the $\bar{N}_p \times \bar{N}_p$ diagonal matrix in which the $k$-th element is the $k$-th SPS in the $i$-th OFDM symbol. The second equality comes from the fact that $\bar{\mathbf{X}}_i^H\bar{\mathbf{X}}_i = \mathbf{I}_{\bar{N}_p}$. Then, the start and end indices of the denoising window, $\alpha$ and $\beta$, can be estimated by minimizing the SE (24).

Because the MED of the channel determines the actual CIR region, the denoising window is highly dependent on it. Under a scenario for the stationary transmitter and receiver with moderate drift, the MED of the channel does not change drastically within the frame duration. Therefore, we propose using a universal denoising window for all OFDM symbols in a given frame. In the proposed denoising window estimation, the SE of all SPSs allocated in a frame is exploited as follows:

$$\begin{aligned}\bar{\varepsilon}(\alpha, \beta) &= \frac{1}{\bar{N}_t}\sum_{i\in\bar{I}_t}\bar{\varepsilon}_i(\alpha, \beta) \\ &= \frac{1}{\bar{N}_t\bar{N}_p}\sum_{i\in\bar{I}_t}||\bar{\mathbf{X}}_i^H\bar{\mathbf{y}}_i - \bar{\mathbf{H}}_i(\alpha, \beta)||_2^2.\end{aligned} \tag{25}$$

Based on (25), the universal denoising window can be estimated as

$$\mathbf{D}_{\alpha,\beta}^{u} = \arg\min_{i,j}\{\bar{\varepsilon}(i, j)\}. \tag{26}$$

If the denoising window overlaps with the actual CIR region, the corresponding tentative CFR is distorted due to loss of the actual channel tap, which will result in an increase in the SE $\bar{\varepsilon}(\alpha, \beta)$. If the denoising window corresponds to only some portion of the noise region, this also results in a high SE. Therefore, the denoising window estimated by (26) will coincide with the largest noise region outside of the actual CIR that minimizes the overall SE in (25). Note that usage of overall SE has the benefit of averaging out noise and

[1] If the SPS is not co-located with PPS ($\bar{I}_t \notin I_t$), the CIR estimate for the OFDM symbol carrying the SPS $\check{\mathbf{h}}_j(j \in \bar{I}_t)$ is obtained firstly by temporal interpolation of the CIR estimates $\tilde{\mathbf{h}}_i(i \in I_t)$, then, the tentative CFR can be acquired as in (23).

**Algorithm 1** The SPS-Aided Denoising Window Estimation

**Input:** $\bar{\mathbf{X}}_i$ and $\bar{\mathbf{y}}_i$ for $\forall i \in \bar{I}_t$

**Output:** The start and end indices of denoising window, $\alpha$ and $\beta$

1) *End Index Determination*

$a = \alpha_{init},\ b = N-1$
$\bar{\mathbf{e}}_i(a,\ b) = \bar{\mathbf{X}}_i^H \bar{\mathbf{y}}_i - \bar{\mathbf{H}}_i(a,\ b),\ \forall i \in \bar{I}_t$
$\bar{\varepsilon}(a,\ b) = \frac{1}{\bar{N}_t \bar{N}_p} \sum_{i \in \bar{I}_t} ||\mathbf{e}_i(a,\ b)||_2^2$
**for** $b = N-2$ to $N - N_b$ **do**
  $\bar{\mathbf{e}}_i(a,\ b) = \bar{\mathbf{e}}_i(a,\ b+1) - \sqrt{N}\tilde{h}_i(b+1)\bar{\mathbf{b}}_{b+1},\ \forall i \in \bar{I}_t$
  $\bar{\varepsilon}(a,\ b) = \frac{1}{\bar{N}_t \bar{N}_p} \sum_{i \in \bar{I}_t} ||\bar{\mathbf{e}}_i(a,\ b)||_2^2$
**end for**
$\beta \leftarrow \arg\min_b \{\bar{\varepsilon}(a,\ b)\},\ b = N - N_b, \cdots, N-1$

2) *Start Index Determination*

$a = \alpha_{init}$
$\bar{\mathbf{e}}_i(a,\ \beta) = \bar{\mathbf{X}}_i^H \bar{\mathbf{y}}_i - \bar{\mathbf{H}}_i(a,\ \beta),\ \forall i \in \bar{I}_t$
$\bar{\varepsilon}(a,\ \beta) = \frac{1}{\bar{N}_t \bar{N}_p} \sum_{i \in \bar{I}_t} ||\mathbf{e}_i(a,\ \beta)||_2^2$
**for** $a = \alpha_{init} - 1$ to $\alpha_{init} - N_a$ **do**
  $\bar{\mathbf{e}}_i(a,\ \beta) = \bar{\mathbf{e}}_i(a+1,\ \beta) + \sqrt{N}\tilde{h}_i(a)\bar{\mathbf{b}}_a,\ \forall i \in \bar{I}_t$
  $\bar{\varepsilon}(a,\ \beta) = \frac{1}{\bar{N}_t \bar{N}_p} \sum_{i \in \bar{I}_t} ||\bar{\mathbf{e}}_i||_2^2$
  $a \leftarrow a+1$
**end for**
$\alpha \leftarrow \arg\min_a \{\bar{\varepsilon}(a,\ \beta)\},\ a = \alpha_{init} - N_a, \cdots, \alpha_{init}$

undesired fluctuations in the SE, thereby achieving improved accuracy.

In (26), $\bar{\varepsilon}(\alpha, \beta)$ is a 2-D function of the start and end indices of a denoising window. One can find the minimum of $\bar{\varepsilon}(\alpha, \beta)$ with a 2-D exhaustive greedy search. However, this requires huge computational complexity because the ranges of $\alpha$ and $\beta$ are large ($0 \le \alpha, \beta \le N-1$). Therefore, we adopt a two-step approach, in which the end index of the denoising window is first estimated for a fixed value of the start index, and based on the estimated end index, the start index is searched in a similar way.

Let $\bar{\mathbf{e}}_i(a,\ b) = \bar{\mathbf{X}}_i^H \bar{\mathbf{y}}_i - \bar{\mathbf{H}}_i(a,\ b),\ i \in \bar{I}_t$ denote the $\bar{N}_p \times 1$ error vector for the SPSs in the $i$-th OFDM symbol for a given denoising window $\mathbf{D}(a,\ b)$. Then, $\bar{\varepsilon}(a,\ b)$ can be rewritten as

$$\bar{\varepsilon}(a,\ b) = \frac{1}{\bar{N}_t \bar{N}_p} \sum_{i \in \bar{I}_t} ||\bar{\mathbf{e}}_i(a,\ b)||_2^2. \tag{27}$$

It is important to note that for a fixed value of $a$, $\bar{\mathbf{e}}_i(a,\ b)$ can be obtained from $\bar{\mathbf{e}}_i(a,\ b+1)$ by recovering the contribution of the $(b+1)$-th element of $\tilde{\mathbf{h}}_i$ as

$$\begin{aligned}\bar{\mathbf{e}}_i(a,\ b) &= \bar{\mathbf{X}}_i^H \bar{\mathbf{y}}_i - \left(\bar{\mathbf{H}}_i(a,\ b+1) + \sqrt{N}[\tilde{h}_i]_{b+1}\bar{\mathbf{b}}_{b+1}\right) \\ &= \bar{\mathbf{e}}_i(a,\ b+1) - \sqrt{N}[\tilde{h}_i]_{b+1}\bar{\mathbf{b}}_{b+1}\end{aligned} \tag{28}$$

where $\bar{\mathbf{b}}_k$ is the $k$-th column vector of $\bar{\mathbf{B}}$. Accordingly, $\bar{\mathbf{e}}_i(a,\ b)$ and the corresponding $\bar{\varepsilon}(a,\ b)$ can be readily computed in a recursive way for a decreasing $b$ with a fixed value of $a$. End index $\beta$ is then determined from the minimum of $\bar{\varepsilon}(a,\ b)$.

Similarly, $\bar{\mathbf{e}}_i(a,\ \beta)$ can be computed from $\bar{\mathbf{e}}_i(a+1,\ \beta)$ as

$$\begin{aligned}\bar{\mathbf{e}}_i(a,\ \beta) &= \bar{\mathbf{X}}_i^H \bar{\mathbf{y}}_i - \left(\bar{\mathbf{H}}_i(a+1,\ \beta) - \sqrt{N}[\tilde{h}_i]_a\bar{\mathbf{b}}_a\right) \\ &= \bar{\mathbf{e}}_i(a+1,\ \beta) + \sqrt{N}[\tilde{h}_i]_a\bar{\mathbf{b}}_a.\end{aligned} \tag{29}$$

Based on the determined $\beta$, $\bar{\mathbf{e}}_i(a,\ \beta)$ and the corresponding $\bar{\varepsilon}(a,\ \beta)$ are again computed recursively, based on which start index $\alpha$ is determined from the minimum. Since $\bar{\mathbf{e}}_i(a,\ b)$ is updated recursively, the proposed SPS-aided denoising window estimation has low complexity. The proposed method is summarized in Algorithm 1, where $N_a$ and $N_b$ account for the search range of $\alpha$ and $\beta$, respectively, and $\alpha_{init}$ is the initial value of $\alpha$.

## IV. PERFORMANCE ANALYSIS

### A. EFFECT OF DENOISING

In order to investigate the effect of denoising on a noisy CIR estimate, we consider the MSE of the CIR for a given denoising window with $\alpha$ and $\beta$ as

$$\begin{aligned}\sigma_e^2(\alpha, \beta) &= E\left[\left\|\mathbf{h} - \check{\mathbf{h}}\right\|_2^2\right] \\ &= tr\left(E\left[\mathbf{e}_h\mathbf{e}_h^H\right]\right)\end{aligned} \tag{30}$$

where

$$\begin{aligned}\mathbf{e}_h &= \mathbf{h} - \check{\mathbf{h}} \\ &= \Omega_{\alpha,\beta}\mathbf{h} - \frac{1}{\sqrt{N}}\mathbf{D}_{\alpha,\beta}\Psi\mathbf{w},\end{aligned} \tag{31}$$

$\Psi = \mathbf{Q}^H\Gamma\mathbf{B}$, and $\Omega_{\alpha,\beta} = \mathbf{I}_N - \mathbf{D}_{\alpha,\beta}\Psi$. In (30), for ease of analysis, the thresholding is ignored by letting $\Xi = \mathbf{I}_N$, the subscript $i$ for the CIR estimate is dropped, and the interpolation with the LI matrix $\Gamma$ in (14) is considered. After some algebraic manipulations, the MSE of (30) becomes

$$\sigma_e^2(\alpha, \beta) = tr\left(\Omega_{\alpha,\beta}\mathbf{C}_h\Omega_{\alpha,\beta}^H\right) + \frac{\sigma_n^2}{N}tr\left(\mathbf{D}_{\alpha,\beta}\Psi\Psi^H\mathbf{D}_{\alpha,\beta}^H\right). \tag{32}$$

In (32), the first term corresponds to inaccuracy of the estimator and can be rewritten as

$$tr\left(\Omega_{\alpha,\beta}\mathbf{C}_h\Omega_{\alpha,\beta}^H\right) = \sum_{l=0}^{N-1} ||\mathrm{col}_l\left(\Omega_{\alpha,\beta}\right)||_2^2\,\sigma_l^2. \tag{33}$$

We can see from (33) that the first term is represented as a sum of the variance of each channel tap, weighted by the norm of the corresponding column vector of $\Omega_{\alpha,\beta}$. The second term of the MSE in (32) corresponds to a variance of the noise colored by the estimator $\Psi_{\alpha,\beta}$, and can be rewritten as

$$\frac{\sigma_n^2}{N}tr\left(\mathbf{D}_{\alpha,\beta}\Psi\Psi^H\mathbf{D}_{\alpha,\beta}^H\right) = \frac{\sigma_n^2}{N}\sum_{l=0}^{N-1}[\mathbf{D}_{\alpha,\beta}]_{l,l}||\mathrm{row}_l\left(\Psi\right)||_2^2. \tag{34}$$

First, when the channel tap is removed by the denoising window, the first term of the MSE increases due to lack of an estimate of the corresponding tap. In the appendix,

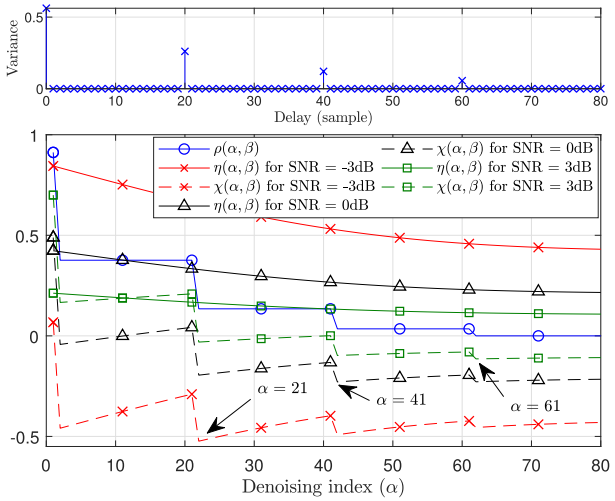


**FIGURE 2.** $\rho(\alpha, \beta)$, $\eta(\alpha, \beta)$ and $\chi(\alpha, \beta)$ according to $\alpha$ for SNR = -3 dB, 0 dB, and 3 dB. $\beta$ is set to 511.

**TABLE 1.** Parameters of the UWA CP-OFDM system for the simulation and the experiment.

| | | |
|---|---|---|
| Bandwidth | $B$ | 5 kHz |
| Carrier frequency | $f_c$ | 12 kHz |
| No. of total subcarriers | $N$ | 512 |
| No. of useful subcarriers | $N_U$ | 400 |
| No. of null subcarriers | $N_g$ | 109 |
| No. DC subcarriers | $N_{DC}$ | 3 |
| Spacing for PPS in frequency and time | $[D_f,\ D_t]$ | [4, 1] |
| Spacing for SPS in frequency and time | $[\bar{D}_f,\ \bar{D}_t]$ | [25, 1] |
| No. of repetitions in the frequency domain | $N_{rep}$ | 1, 4 |
| No. of preambles | $N_{preamble}$ | 2 |
| No. of OFDM symbols | $N_{sym}$ | 54 |
| OFDM block duration | $T_b$ | 125 ms |
| CP duration | $T_{CP}$ | 22.6 ms |
| Frame duration | $T_{frame}$ | 7 s |

the increment of the MSE by discarding the channel tap with a delay of $\tau$, i.e., $\alpha = \tau$, is derived as

$$a(\tau) \simeq \left(2\Re\left\{[\Psi]_{\tau,\tau}\right\} - \left|[\Psi]_{\tau,\tau}\right|^2\right)\sigma_l^2. \tag{35}$$

On the other hand, noise is contained in all elements of the noisy CIR estimate. Accordingly, discarding any element removes the noise, thereby reducing the second term of the MSE. It can readily be derived from (34) that a decrease in the second term of the MSE by removing the $\tau$-th element of the noisy CIR estimate is equivalent to the norm of the $\tau$-th row vector of $\Psi$, which is given by

$$b(\tau) = \frac{\sigma_n^2}{N}||\text{row}_\tau(\Psi)||_2^2 = \frac{\sigma_n^2}{N}\sum_{k=0}^{N-1}\left|[\Psi]_{\tau,k}\right|^2. \tag{36}$$

Compared with the MSE with no denoising, an overall change in MSE by a denoising window with a given $\alpha$ and $\beta$ is equivalent to the difference between the cumulative sum of $a(l)$ and $b(l)$ for $\alpha \le l \le \beta$ as

$$\begin{aligned}\chi(\alpha,\beta) &= \sigma_e^2(\alpha,\beta) - \sigma_e^2(N,N)\\ &= \rho(\alpha,\beta) - \eta(\alpha,\beta),\end{aligned} \tag{37}$$

where $\rho(\alpha,\beta) = \sum_{l=\alpha}^{\beta} a(l)$, and $\eta(\alpha,\beta) = \sum_{l=\alpha}^{\beta} b(l)$. Note that $\chi(\alpha,\beta)$ should be negative to obtain the gain from denoising. Therefore, the optimal denoising indices $\alpha^*$ and $\beta^*$ are the ones that reach the minimum of $\chi(\alpha,\beta)$ from the MSE perspective:

$$\left\{\alpha^*, \beta^*\right\} = \arg\min_{\alpha,\beta}\left\{\chi(\alpha,\beta)\right\}. \tag{38}$$

In the upper side of Fig. 2, the power delay profile of a channel is shown as a toy example. In the lower side of Fig. 2, $\rho(\alpha,\beta)$, $\eta(\alpha,\beta)$, and $\chi(\alpha,\beta)$ are depicted as a function of $\alpha$ with a fixed value of $\beta = 511$ for various SNRs (−3 dB, 0 dB, and 3 dB). The parameters of the UWA CP-OFDM system used in Fig. 2 are summarized in Table 1. The details of the parameters will be discussed in the section V. Note that $\rho(\alpha,\beta)$ depends only on the power delay profile and is independent of SNR, while $\eta(\alpha,\beta)$ depends only on SNR.

We see that $\eta(\alpha,\beta)$ is a monotonically decreasing function scaled with noise variance $\sigma_n^2$, whereas $\rho(\alpha,\beta)$ is also a decreasing function with abrupt changes owing to channel taps. The results reveal that the minimum value of $\chi(\alpha,\beta)$ is determined by $\eta(\alpha,\beta)$, while the shape of $\chi(\alpha,\beta)$ is largely affected by $\rho(\alpha,\beta)$. We also observe that $\chi(\alpha,\beta)$ reaches the minimum at $\alpha = 21$, $\alpha = 41$, and $\alpha = 61$ for SNRs of −3 dB, 0 dB and 3 dB, respectively. Note that $\alpha = 21$, $\alpha = 41$, and $\alpha = 61$ correspond to the delay next to the second, third, and fourth taps of the exemplary channel, respectively. This indicates the following: for a low SNR regime, discarding large portions of the noisy channel estimate is advantageous, despite sacrificing the estimates of small channel taps, whereas as SNR increases, maintaining the estimates of small channel taps becomes important.

### B. PERFORMANCE ANALYSIS FOR THE SPS-AIDED DENOISING WINDOW ESTIMATION

The accuracy of the proposed SPS-aided denoising window estimator is analyzed and compared with that of the optimal denoising window obtained numerically by an exhaustive search. In order to investigate performance of the proposed method for the channel with various statistics, we consider a spare channel with $N_{path} = 8$ taps having a random delay. In particular, the delay of each path is randomly distributed within 15 ms, where the minimum difference in time between adjacent paths is set to 1 ms. The amplitude of each path is drawn from a Rayleigh distribution, where the path gain decreases exponentially, with the difference between the first and the last paths being 25 dB. No Doppler rate for each path is considered ($a_l = 0$). The UWA CP-OFDM system with the same parameters in Table 1 is used for the numerical analysis.

For a performance metric, the MSE and the relative difference between the SEs of the CFR estimate over the useful

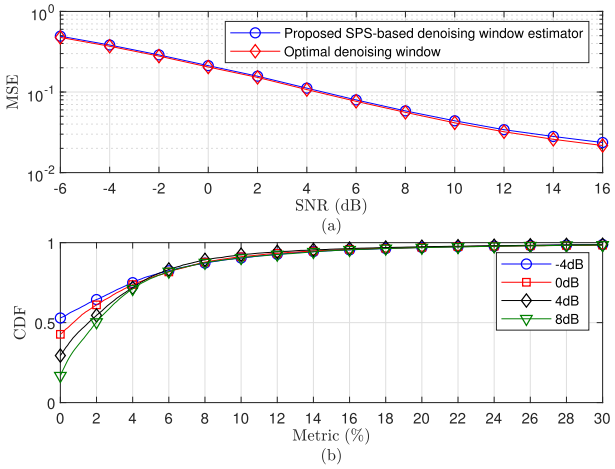


**FIGURE 3.** Performance comparison between the proposed and optimal estimation of the denoising window indices: (a) the MSE in (41), and (b) the CDF of the relative difference between SEs in (42).

subcarriers are considered. Without considering the thresholding $\Xi$ (17) and the adaptive temporal filtering (22), the CFR estimate for a given denoising window with indices $\alpha$ and $\beta$ is given by

$$\check{\mathbf{H}}_i(\alpha, \beta) = \sqrt{N}\mathbf{Q}\mathbf{D}_{\alpha,\beta}\tilde{\mathbf{h}}_i, \quad i \in I_t. \tag{39}$$

The SE of the CFR estimate over the useful subcarriers is then represented as

$$\epsilon(\alpha, \beta) = \frac{1}{N_U N_t} \sum_{i \in I_t} ||\mathbf{H} - \check{\mathbf{H}}_i(\alpha, \beta)||_2^2 \tag{40}$$

where $\mathbf{H} = \mathbf{Q}\mathbf{h}$ is an actual CFR vector over the useful subcarriers. The MSE is defined as

$$\text{MSE} = E\left[\varepsilon(\alpha, \beta)\right] = E\left[||\mathbf{H} - \check{\mathbf{H}}_i(\alpha, \beta)||_2^2\right], \quad \forall i. \tag{41}$$

The relative difference between SEs with the proposed and optimal indices is defined as

$$\text{Metric} = \frac{\epsilon(\alpha, \beta) - \epsilon(\alpha^*, \beta^*)}{\epsilon(\alpha^*, \beta^*)} \times 100 \tag{42}$$

where $\alpha^*$ and $\beta^*$ are the start and end indices, respectively, of the optimal denoising window.

Fig. 3(a) and Fig. 3(b) show the performance comparison between the proposed and the optimal estimation of the denoising window for the MSE and the cumulative distribution function (CDF) of the metric in (42), respectively. It is seen from Fig. 3(a) that the proposed method is capable of estimating the near-optimal denoising window in the MSE sense. Fig. 3(b) shows that the denoising window obtained by the proposed method yields an SE of the CFR estimate very close to that of the optimal window for all considered SNR values. Specifically, in Fig. 3(b), we have a 90% probability for all considered SNRs that the relative difference between the SEs is less than 10%.

Interestingly, it is observed that the probability that the relative difference is very small ($< 4\%$) is higher for a lower valued SNR. This is due to the shape of $\chi(\alpha, \beta)$ illustrated in Fig.2. In the low SNR regime, the difference between the local and global minimum of $\chi(\alpha, \beta)$ is negligible, whereas the difference grows as SNR increases. As a result, wrong selection of the local minimum in a high SNR regime causes a relatively larger SE, leading to an increase in the metric.

## V. SIMULATION RESULTS

The performance of the proposed CE is evaluated and compared with existing techniques for a UWA CP-OFDM system with the parameters in Table 1. A frame consists of two preambles and 54 OFDM symbols, where each has a duration of 125 ms. Accordingly, a frame has duration of 7 s. The preambles are employed for time and frequency synchronization. A transmitted message for a frame is turbo-coded with a code rate of $1/3$ and modulated by either QPSK and 16QAM constellations. In order to ensure error-free communications at a low SNR, the modulated symbols are repeated in the frequency domain at the cost of reduced spectral efficiency. The repetition of data symbols allows investigation of the robustness of the CE against strong noise, especially in a low SNR regime. In the frequency domain, the PPS and SPS are allocated at every fourth and 25-th subcarriers, respectively ($D_f = 4$ and $\bar{D}_f = 25$). For accurate channel estimation under a time-varying underwater channel, all OFDM symbols carry PPS and SPS, i.e. $D_t = \bar{D}_t = 1$. Note that the SPSs occupy only 4% of the useful subcarriers in each OFDM symbols ($\bar{N}_p/N_U = 16/400 = 0.04$), which incurs a very small overhead.

For the proposed CE, LI and PCHIP are employed for spectral interpolation. and $\gamma$ and $\lambda$ are set to 4 and 0.3, respectively. For the SPS-aided denoising window estimation, $\alpha_{init}$, $N_a$, and $N_b$ are set to 113, 50, and 60, respectively. The denoising window of the conventional LI method with a fixed denoising window is set to discard all elements of the noisy CIR estimate outside of CP region, i.e., $\alpha = 113$ and $\beta = 511$. The same channel described in IV-B, which has a random delay for each path, is considered to reflect the performance under diverse underwater environments.

### A. BLER PERFORMANCE

For performance evaluation under a time-varying channel, the block error rate (BLER) is used as the performance metric, which is defined by the average number of error-free frames after decoding. The Doppler rate of each path is set to $a_l = v_p/c$, where $v_p$ is the relative speed between transmitter and receiver and has an uniform distribution with standard velocity deviation of 0.1 m/s, and $c(= 1500\text{m/s})$ is the sound speed.

Fig. 4, Fig. 5 and Fig. 6, respectively, show the BLER performance for QPSK modulation with frequency repetitions of $N_{rep} = 4$ and $N_{rep} = 1$, and 16QAM modulation with frequency repetitions of $N_{rep} = 1$. Note that the performance of the proposed method without the thresholding and smoothing ($\gamma = 0$ and $\lambda = 1$) is also provided to verify the performance of the adaptive denoising window.

**TABLE 2. Complexity comparison.**

| Method | Number of real multiplications | Example |
|---|---|---|
| Conv. LI [24] | $2\left(N_p+N_U\right)N_t+2N_U(N_{sym}-N_t)$ | 54000 |
| Conv. LI [24] with a fixed denoising window | $2\left(N_p+N_U\right)N_t+4N\log_2(N)+2N_U(N_{sym}-N_t)$ | 72432 |
| OMP [8] | $\left((4N_p+2)L_hN_{path}+2N\log_2(N)+N_{path}^4+\left(2+\frac{4}{3}N_p\right)N_{path}^3+(6N_p+1)N_{path}^2+\frac{14}{3}N_pN_{path}\right)N_t+2N_U(N_{sym}-N_t)$ | 26363232 |
| DW-SACoSaMP [15] | The complexity of DW-SACoSaMP is assumed to be the same as that of OMP | 26363232 |
| Proposed method with LI | $2\left(N_p+N_U+N\right)N_t+N_U\left(6N_{sym}-2N_t-4\right)+4N\log_2(N)+\bar{N}_p\left(4\alpha_{init}+2+6(N_a+N_b-2)\right)\bar{N}_t+1$ | 1164657 |

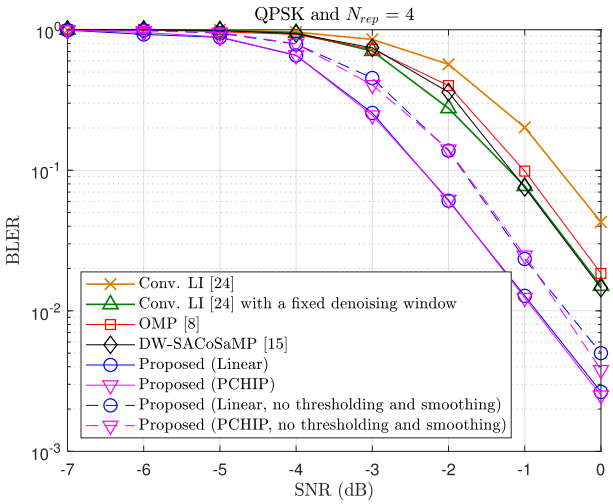


**FIGURE 4. BLER performance versus SNR for QPSK with $N_{rep}=4$.**

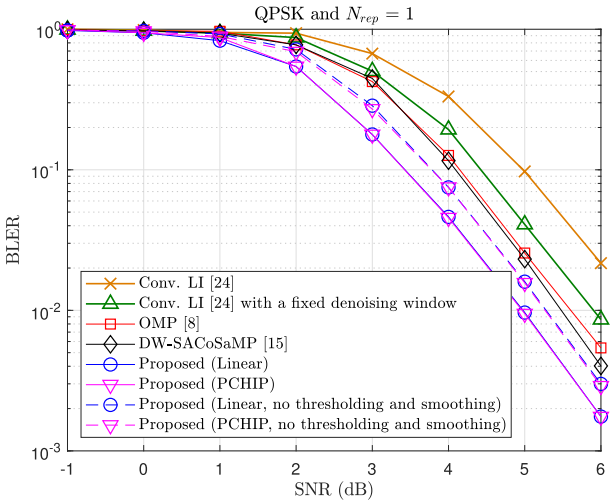


**FIGURE 5. BLER performance versus SNR for QPSK with $N_{rep}=1$.**

In the figures, the performance of the CE methods can be observed for low-, medium-, and high-range of SNRs, respectively. It is seen from Fig. 4 and Fig. 5 that the proposed method shows much better BLER performance than the conventional methods. In particular, the proposed method exhibits a gain of 1 dB and 0.5 dB at BLER = 0.01 over

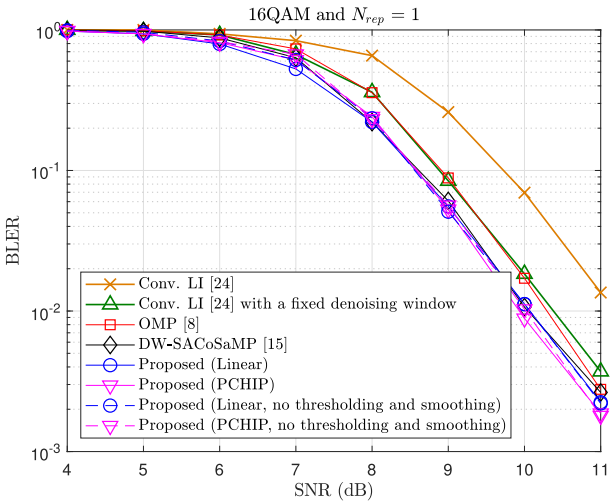


**FIGURE 6. BLER performance versus SNR for 16QAM with $N_{rep}=1$.**

OMP [8] and DW-SACoSaMP [15] in Fig. 4 and Fig. 5, respectively, where the proposed adaptive denoising window gives a gain of 0.5 dB and 0.25 dB, while the thresholding and smoothing provide an additional gain of 0.5 dB and 0.25 dB, respectively. This confirms that the proposed method is capable of suppressing strong noise in channel estimation, thereby enabling reliable underwater communications especially in the low-to-medium SNR regime.

In Fig. 6, the proposed method outperforms OMP with a gain of about 0.3 dB at BLER = 0.01, while the DW-SACoSaMP method has almost the same performance as the proposed method with LI. The proposed method with PCHIP interpolation still shows the best performance for the whole range of SNRs. It is also observed in high SNR scenario that a gain of the proposed method comes solely from the adaptive denoising window. The results in Fig. 6 indicate that the proposed method is able to support a high-order modulation such as 16QAM for UWA communications systems.

### B. COMPLEXITY ANALYSIS

The computational complexity of the proposed CE is analyzed in terms of the number of real multiplications (RMs). Note that complex multiplication costs 4 RMs, and an $N$-point fast Fourier transform operation requires

$2N\log_2(N)$ RMs. First, the LS estimation of CFR in (9) needs 4 $N_pN_t$ RMs, and the spectral interpolation in (10) requires $2(N_U - N_p)N_t$ and $10(N_U - N_p)N_t$ for the LI and PCHIP techniques, respectively. Computation of the noise variance estimate for the thresholding matrix in (18) requires $2NN_t + 1$ RMs. Note that multiplication of the denoising and thresholding matrices cost no RMs. Temporal interpolation and additional smoothing require $2N_U(N_{sym} - N_t)$ and $4N_U(N_{sym} - 1)$ RMs, respectively.

In the SPS-aided denoising window estimation, the number of RMs for initialization of the end index determination (steps 2 and 3) is $(4\alpha_{init} + 2)\bar{N}_p\bar{N}_t$. Then, $6\bar{N}_p\bar{N}_t(N_b - 1)$ RMs are required for steps 5 and 6 for $(N_b - 1)$ iterations. Note that initialization of the start index determination requires no additional computation because all necessary values are computed during the end index determination. Similarly, steps 13 and 14 require $6\bar{N}_p\bar{N}_t(N_a - 1)$ RMs. Therefore, the total complexity for the proposed method is $2\left(N_p + N_U + N\right)N_t + N_U\left(6N_{sym} - 2N_t - 4\right) + 4N\log_2(N) + \bar{N}_p\left(4\alpha_{init} + 2 + 6(N_a + N_b - 2)\right)\bar{N}_t + 1$.

In Table 2, the number of RMs for the CEs is shown. The exemplary values are also provided for the considered UWA CP-OFDM system with the parameters given in Table 1. For OMP [8] and DW-SACoSaMP, matrix inversion is computed at every iteration, which is assumed to require 4 $K^3$ RMs, where $K$ denotes the dimension of the matrix. The number of iterations in the OMP method is set to $N_{path}$, which is equal to the sparsity level of the CIR. In DW-SACoSaMP, it is intractable to analyze the exact complexity, because the number of iterations and the required computations per iteration change [15]. As DW-SACoSaMP is in a family of iterative greedy pursuit algorithms like OMP, the complexity of DW-SACoSaMP is assumed to be the same as that of OMP.[2]

It is seen from the table that OMP and DW-SACoSaMP require more than 20 times greater complexity compared with the proposed method, where huge complexity is mainly from the matrix inversion operation performed at every iteration. Thus, the superior noise suppression capability of the proposed method is highly cost-effective from the perspective of computational complexity.

## VI. EXPERIMENTAL RESULTS

An at-sea experiment was conducted in the Western Sea of Korea near Deokjeok island from 5 July to 6 July, 2017. A UWA CP-OFDM system with the same parameters in Table 1 was used. A frame with a duration of 7 s was transmitted periodically during those 24 hours. The transmitter and receiver were equipped with a single transducer and a hydrophone, respectively. The transducer and hydrophone were submerged to a depth of 20 m and 5 m from sea level, respectively. Both ships for the transmitter and receiver were anchored with a communication range of 2.2km.

[2]It is observed in the simulation that measured complexity of DW-SACoSaMP is slightly smaller than that of OMP.

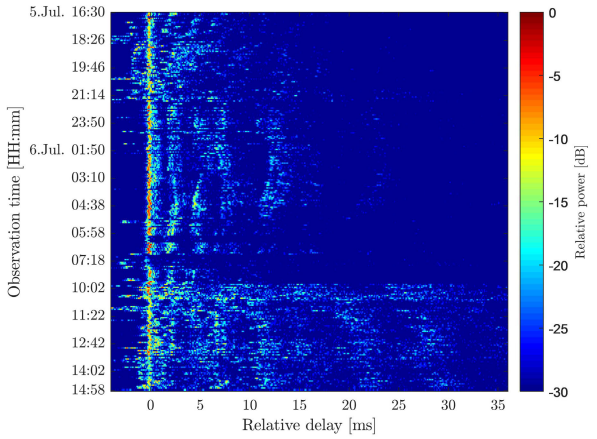


**FIGURE 7.** Underwater CIR measured from 5 July, 16:30, to 6 July, 14:58.

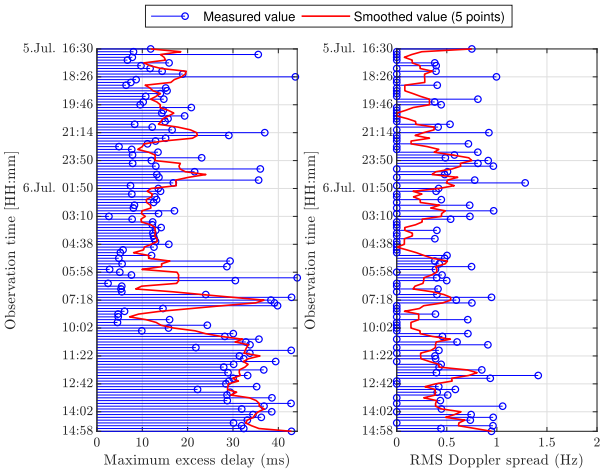


**FIGURE 8.** Estimated MED and RMS DS.

In the experimental area, the strength and direction of the tidal current change rapidly over time. As a result, both ships experienced intermittent drifting caused by the tidal current. Drift induces a weak to mild Doppler effect on the received signal. In addition, the difference in sea level between high and low tides is huge in that area. Consequently, depth was measured at between 35 m and 45 m during the experiment.

### A. MEASURED CIR AND DOPPLER SPREAD OVER TIME

During the experiment, a pseudorandom binary sequence was transmitted periodically for the purpose of measuring the channel response and the Doppler spread over time [25]. Fig. 7 shows the CIR of the underwater channel measured from 5 July at 16:30 to 6 July at 14:58. It is clearly seen that the number of distinct paths and the delay of paths change over time. This is mainly due to the environmental changes in the area, such as tidal current and sea level. It is also observed that the number of distinct paths is not small, while the MED is large. This can be explained by the fact that the experimental site is very shallow compared to the horizontal distance, and has a sandy mud bottom.

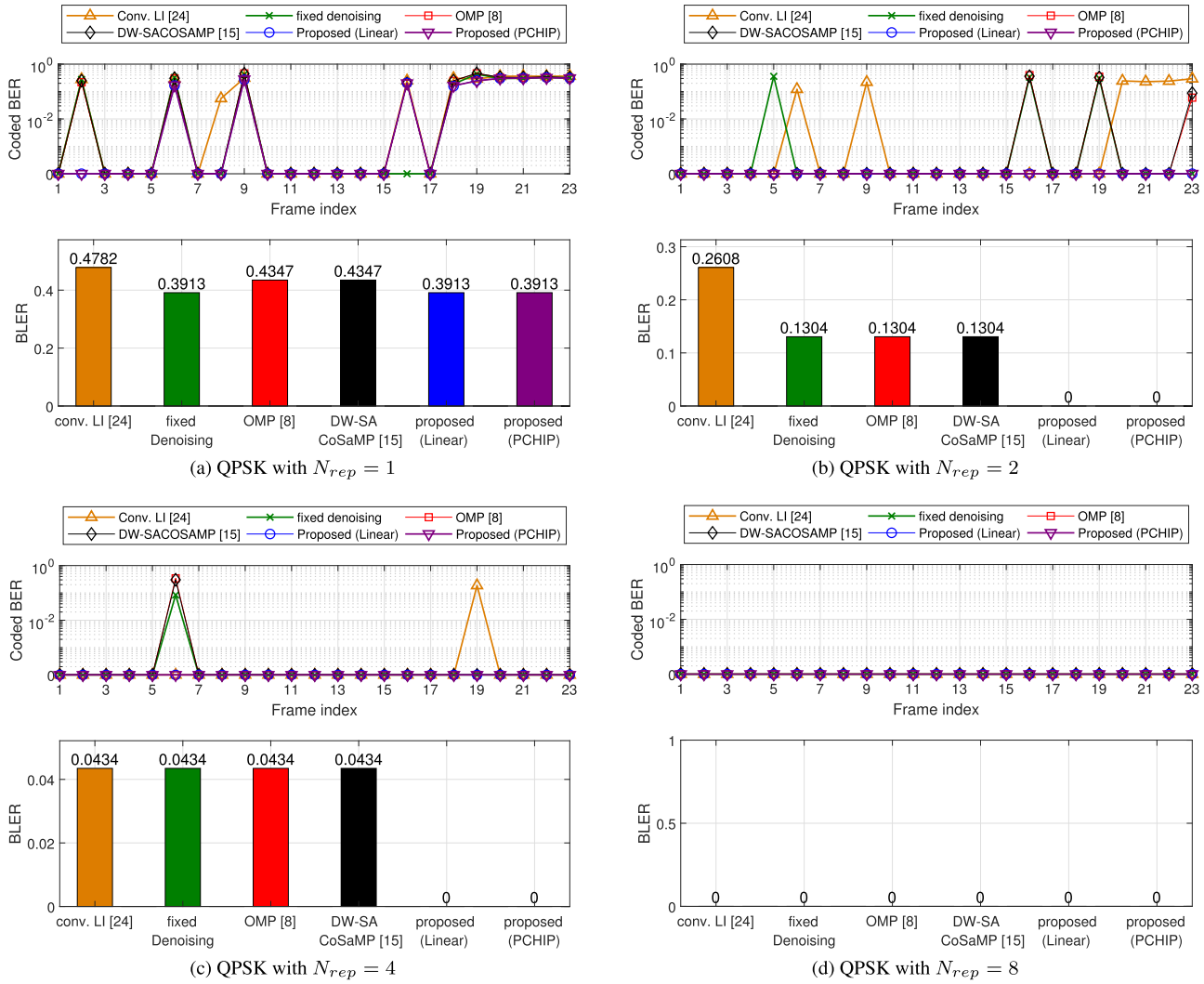


(a) QPSK with $N_{rep} = 1$

(b) QPSK with $N_{rep} = 2$

(c) QPSK with $N_{rep} = 4$

(d) QPSK with $N_{rep} = 8$

**FIGURE 9.** Coded BER and BLER performance for QPSK with frequency repetitions of (a) $N_{rep} = 1$, (b) $N_{rep} = 2$, (c) $N_{rep} = 4$, and (d) $N_{rep} = 8$.

In Fig. 8, the estimated MED of the CIR and the root mean square (RMS) Doppler spread (DS) are depicted, for which smoothed values are also presented. The MED is estimated directly from the measured CIR with a threshold level of $-15$ dB. The RMS DS is estimated based on a scattering function [25]. It is observed that the MED of the channel experiences some noticeable changes during the experiment, in which it remains between 10 ms to 20 ms until the early morning of 6 July, then has short-term increase, and rises to about 30 ms until the end of the experiment. Unlike the MED of the CIR, the RMS DS shows no significant variations, exhibiting a value smaller than 1 Hz in most cases.

### B. CODED BER AND BLER PERFORMANCE FOR QPSK AND 16QAM

To assess the performance for a wide range of SNRs under severe channel variations, four different numbers of repetitions for transmitting data symbols were adopted for the experiment, i.e., $N_{rep} = [1,\ 2,\ 4,\ 8]$. Coded BER and BLER are employed as the performance metric, where the coded BER is defined as BER after channel decoding. Fig. 9(a)-(d) and Fig. 10(a)-(d) show coded BER and BLER performance with various values of $N_{rep}$ for QPSK and 16QAM modulations, respectively. A total of 23 and 22 frames were acquired for the QPSK and 16QAM modulations, respectively.

We observe from Fig. 9 and 10 that the performance of all considered CE methods improves with increasing numbers of frequency repetitions. In QPSK modulation, all methods reaches perfect transmission for the maximum number of repetitions ($N_{rep} = 8$). In 16QAM modulation, however, degradation in performance is observed compared with QPSK modulation, which is due to the increased order of modulation.

We can see from the results that the proposed method outperforms the conventional schemes for all cases of repetitions. For QPSK modulation, the proposed method exhibits perfect transmission (i.e. 0 BLER) except for no repetitions ($N_{rep} = 1$). In 16QAM modulation, the proposed method

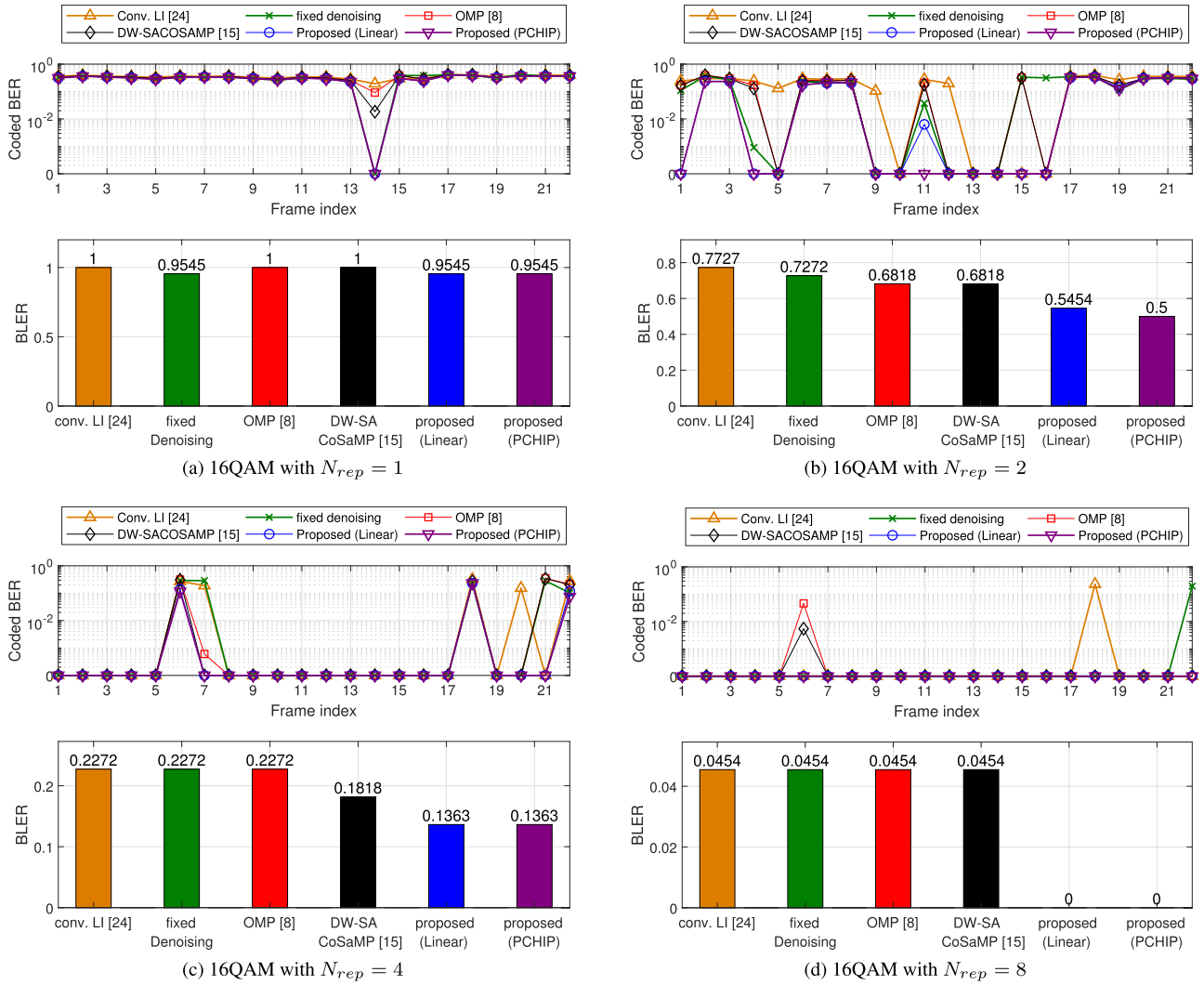


(a) 16QAM with $N_{rep} = 1$

(b) 16QAM with $N_{rep} = 2$

(c) 16QAM with $N_{rep} = 4$

(d) 16QAM with $N_{rep} = 8$

**FIGURE 10.** Coded BER and BLER performance for 16QAM with frequency repetitions of (a) $N_{rep} = 1$, (b) $N_{rep} = 2$, (c) $N_{rep} = 4$, and (d) $N_{rep} = 8$.

only reaches perfect transmission when the maximum frequency repetition is applied. This superior performance can achieve a reliable communication links and lead to a reduction in retransmissions, which saves power consumption and prevents resultant delays caused by unnecessary retransmissions. Furthermore, the improved performance of the proposed method enables transmissions with lower power on the transmitter side. In particular, low power consumption is crucial for UWA communications systems, not only because of limited battery life, but also the huge cost of, and difficulty with, battery replacement. Another advantage of the proposed method is that its enhanced performance allows transmission with a lower number of repetitions, thereby achieving a higher data rate for underwater communications systems. It is worth noting that the performance of the proposed method is obtained without any adjustment of the relevant parameters. Therefore, the proposed method can enable the operation of UWA communications systems under various channel environments.

## VII. CONCLUSION

In this article, a CE method based on an adaptive denoising technique is proposed for a UWA CP-OFDM system in order to overcome strong noise and a harsh underwater channel. By minimizing the SE of the received SPSs, the proposed SPS-aided denoising window estimator is capable of determining the denoising region adaptively according to the channel length of a given CIR estimate. As a result, the proposed method does not need any a priori information about channel statistics and SNR values. Performance analysis verifies that the proposed denoising window estimator can yield the near-optimal denoising window with a very small number of SPSs. It is shown by simulation results that, in comparison to the conventional CEs, the proposed method achieves higher accuracy in the estimation for a time-varying UWA channel, especially in a low SNR regime. The superiority of the proposed method is also confirmed by the at-sea experiment, in which the proposed method yields the lowest BLER for received signals recorded over a 24-hour

period. Complexity analysis show that the proposed method has a much lower complexity compared with the conventional CS-based CEs, because it can be implemented without involving a computationally intensive matrix inversion. Therefore, the proposed method is feasible and effective for a real-time UWA CP-OFDM system under a UWA channel with diverse environmental conditions.

## APPENDIX

When the start index of a denoising window coincides with the delay of a channel tap, the corresponding tap is discarded. The increment of the first term of the MSE by discarding a channel tap with a delay of $\tau$ is the difference between the MSEs before and after discarding the tap:

$$\begin{aligned} a(\tau) &= \sigma_a^2(\tau,\beta) - \sigma_a^2(\tau+1,\beta) \\ &= \sum_{l=0}^{N-1} \left( ||\mathrm{col}_l\left(\Omega_{\tau,\beta}\right)||_2^2 - ||\mathrm{col}_l\left(\Omega_{\tau+1,\beta}\right)||_2^2 \right) \sigma_l^2. \end{aligned} \tag{43}$$

For a given denoising window with $\alpha$ and $\beta$, $||\mathrm{col}_l\left(\Omega_{\alpha,\beta}\right)||_2^2$ can be rewritten as

$$\begin{aligned} &||\mathrm{col}_l\left(\Omega_{\alpha,\beta}\right)||_2^2 \\ &= \sum_{k=0,k\neq l}^{N-1} \left[\mathbf{D}_{\alpha,\beta}\right]_{k,k} \left|[\Psi]_{k,l}\right|^2 + \left|1 - \left[\mathbf{D}_{\alpha,\beta}\right]_{l,l} [\Psi]_{l,l}\right|^2 \\ &\simeq \left|1 - \left[\mathbf{D}_{\alpha,\beta}\right]_{l,l} [\Psi]_{l,l}\right|^2 \end{aligned} \tag{44}$$

where the first term is ignored because estimator $\Psi$ is a diagonal-like matrix. Substituting (44) into (43) yields

$$\begin{aligned} &a(\tau) \\ &\simeq \sum_{l=0}^{N-1} \left( \left|1 - \left[\mathbf{D}_{\tau,\beta}\right]_{l,l} [\Psi]_{l,l}\right|^2 - \left|1 - \left[\mathbf{D}_{\tau+1,\beta}\right]_{l,l} [\Psi]_{l,l}\right|^2 \right) \sigma_l^2. \end{aligned} \tag{45}$$

Note that $\left[\mathbf{D}_{\tau,\beta}\right]_{l,l}$ and $\left[\mathbf{D}_{\tau+1,\beta}\right]_{l,l}$ are identical for all $l$ except for $l=\tau$, in that $\left[\mathbf{D}_{\tau,\beta}\right]_{\tau,\tau} = 0$ and $\left[\mathbf{D}_{\tau+1,\beta}\right]_{\tau,\tau} = 1$. Accordingly, we have

$$\begin{aligned} &a(\tau) \\ &\simeq \left( \left|1 - \left[\mathbf{D}_{\tau,\beta}\right]_{\tau,\tau} [\Psi]_{\tau,\tau}\right|^2 - \left|1 - \left[\mathbf{D}_{\tau+1,\beta}\right]_{\tau,\tau} [\Psi]_{\tau,\tau}\right|^2 \right) \sigma_l^2 \\ &= \left(1 - \left|1 - [\Psi]_{\tau,\tau}\right|^2\right) \sigma_l^2 \\ &= \left(2\Re\left\{[\Psi]_{\tau,\tau}\right\} - \left|[\Psi]_{\tau,\tau}\right|^2\right) \sigma_l^2. \end{aligned} \tag{46}$$

## REFERENCES


[1] M. Chitre, S. Shahabudeen, and M. Stojanovic, "Underwater acoustic communications and networking: Recent advances and future challenges," *Mar. Technol. Soc. J.*, vol. 42, no. 1, pp. 103–116, Mar. 2008.

[2] S. Sendra, J. Lloret, J. M. Jimenez, and L. Parra, "Underwater acoustic modems," *IEEE Sensors J.*, vol. 16, no. 11, pp. 4063–4071, Jun. 2016.

[3] Z. Zeng, S. Fu, H. Zhang, Y. Dong, and J. Cheng, "A survey of underwater optical wireless communications," *IEEE Commun. Surveys Tuts.*, vol. 19, no. 1, pp. 204–238, 1st Quart., 2017.

[4] Y. Li, S. Wang, C. Jin, Y. Zhang, and T. Jiang, "A survey of underwater magnetic induction communications: Fundamental issues, recent advances, and challenges," *IEEE Commun. Surveys Tuts.*, vol. 21, no. 3, pp. 2466–2487, 3rd Quart., 2019.

[5] A. C. Sing, J. K. Nelson, and S. S. Kozat, "Signal processing for underwater acoustic communications," *IEEE Commun. Mag.*, vol. 47, no. 1, pp. 90–96, Jan. 2009.

[6] M. Stojanovic and J. Preisig, "Underwater acoustic communication channels: Propagation models and statistical characterization," *IEEE Commun. Mag.*, vol. 47, no. 1, pp. 84–89, Jan. 2009.

[7] R. V. Nee and R. Prasad, *OFDM for Wireless Multimedia Communications*. Norwood, MA, USA: Artech House, 2000.

[8] C. Berger, S. Zhou, J. Preisig, and P. Willett, "Sparse channel estimation for multicarrier underwater acoustic communication: From subspace methods to compressed sensing," *IEEE Trans. Signal Process.*, vol. 58, no. 3, pp. 1708–1721, Mar. 2010.

[9] C. Qi, X. Wang, and L. Wu, "Underwater acoustic channel estimation based on sparse recovery algorithms," *IET Signal Process.*, vol. 5, no. 8, pp. 739–747, 2011.

[10] Y. Huang, L. Wan, S. Zhou, Z. Wang, and J. Huang, "Comparison of sparse recovery algorithms for channel estimation in underwater acoustic OFDM with data-driven sparsity learning," *Phys. Commun.*, vol. 13, pp. 156–167, Dec. 2014.

[11] Y. Chen, C. Clemente, J. Soraghan, and S. Weiss, "Fractional Fourier based sparse channel estimation for multicarrier underwater acoustic communication system," in *Proc. Sensor Signal Process. Defence (SSPD)*, Sep. 2016, pp. 1–5.

[12] C. Li, K. Song, and L. Yang, "Low computational complexity design over sparse channel estimator in underwater acoustic OFDM communication system," *IET Commun.*, vol. 11, no. 7, pp. 1143–1151, May 2017.

[13] Z. Wang, H. Wu, and S. Liu, "An improved sparse underwater acoustic OFDM channel estimation method based on joint sparse model and exponential smoothing," in *Proc. IEEE Int. Conf. Signal Process., Commun. Comput. (ICSPCC)*, Oct. 2017, pp. 1–6.

[14] P. Chen, Y. Rong, S. Nordholm, Z. He, and A. J. Duncan, "Joint channel estimation and impulsive noise mitigation in underwater acoustic OFDM communication systems," *IEEE Trans. Wireless Commun.*, vol. 16, no. 9, pp. 6165–6178, Sep. 2017.

[15] J. Wang, Z. Yan, W. Shi, and X. Yang, "Underwater acoustic sparse channel estimation based on DW-SACoSaMP reconstruction algorithm," *IEEE Commun. Lett.*, vol. 23, no. 11, pp. 1985–1988, Nov. 2019.

[16] E. Panayirci, M. T. Altabbaa, M. Uysal, and H. V. Poor, "Sparse channel estimation for OFDM-based underwater acoustic systems in Rician fading with a new OMP-MAP algorithm," *IEEE Trans. Signal Process.*, vol. 67, no. 6, pp. 1550–1565, Mar. 2019.

[17] A. Radosevic, R. Ahmed, T. M. Duman, J. G. Proakis, and M. Stojanovic, "Adaptive OFDM modulation for underwater acoustic communications: Design considerations and experimental results," *IEEE J. Ocean. Eng.*, vol. 39, no. 2, pp. 357–370, Apr. 2014.

[18] A. Tadayon and M. Stojanovic, "Low-complexity superresolution frequency offset estimation for high data rate acoustic OFDM systems," *IEEE J. Ocean. Eng.*, vol. 44, no. 4, pp. 932–942, Oct. 2019.

[19] Y. Kang, K. Kim, and H. Park, "Efficient DFT-based channel estimation for OFDM systems on multipath channels," *IET Commun.*, vol. 1, no. 2, pp. 197–202, Apr. 2007.

[20] S. Rosati, G. E. Corazza, and A. Vanelli-Coralli, "OFDM channel estimation based on impulse response decimation: Analysis and novel algorithms," *IEEE Trans. Commun.*, vol. 60, no. 7, pp. 1996–2008, Jul. 2012.

[21] H. Xie, G. Andrieux, Y. Wang, J.-F. Diouris, and S. Feng, "Efficient time domain threshold for sparse channel estimation in OFDM system," *AEU-Int. J. Electron. Commun.*, vol. 68, no. 4, pp. 277–281, Apr. 2014.

[22] P. Sure and C. M. Bhuma, "A survey on OFDM channel estimation techniques based on denoising strategies," *Eng. Sci. Technol., Int. J.*, vol. 20, no. 2, pp. 629–636, Apr. 2017.

[23] G. Ren, H. Zhang, and Y. Chang, "SNR estimation algorithm based on the preamble for OFDM systems in frequency selective channels," *IEEE Trans. Commun.*, vol. 57, no. 8, pp. 2230–2234, Aug. 2009.

[24] Y. Acar, H. Doğan, and E. Panayirci, "Pilot symbol aided channel estimation for spatial modulation-OFDM systems and its performance analysis with different types of interpolations," *Wireless Pers. Commun.*, vol. 94, no. 3, pp. 1387–1404, Jun. 2017.

[25] P. van Walree, T. Jenserud, and M. Smedsrud, "A discrete-time channel simulator driven by measured scattering functions," *IEEE J. Sel. Areas Commun.*, vol. 26, no. 9, pp. 1628–1637, Dec. 2008.

**YONG-HO CHO** received the B.S., M.S., and Ph.D. degrees in electrical engineering from the Korea Advanced Institute of Science and Technology (KAIST), Daejeon, South Korea, in 2004, 2006, and 2013, respectively. From 2013 to 2016, he was a Senior Researcher with Samsung Electronics in charge of research and development for 5G and the IoT communication systems. He is currently an Assistant Professor with the Department of Information and Communication Engineering, Hoseo University. His research interests include 5G mobile communication systems, the Internet of Things, underwater communication systems, and deep learning.

**HAK-LIM KO** received the B.S. degree in electronic engineering from Soongsil University, Seoul, South Korea, in 1983, the M.S. degree in electrical engineering from Fairleigh Dickinson University, Teaneck, NJ, USA, in 1986, and the Ph.D. degree in electrical and computer engineering from North Carolina State University, Raleigh, NC, USA, in 1995. Since 1996, he has been with the Department of Information and Communications Engineering, Hoseo University, Asan, South Korea, where he is currently a Professor. His current research interests include underwater communications and array signal processing.